

obtained by Martin [13]. In reducing the original correlation, the applicable parametric ranges were narrowed into those of practical interest in electronics cooling.

3.2.7 Forced convective heat transfer from modules on board

Once mounted on the printed circuit board, heat transfer from the module is affected by the geometric parameters depicted in Fig. 3.10. In addition to the size of the module [b (height) \times l (length) \times w (width)], there are such parameters as the separation distance between the neighboring modules (row spacing s , column spacing s'), the location of the module [in row number n ($1 \leq n \leq N$) counted from the entrance of the coolant channel], and the channel height (H). The real situation is far more complex than that portrayed in Fig. 3.10; particularly in small systems, the geometric regularity in placement of modules and other components exists only to a certain extent. Most of the pertinent data reported in the literature are useful for the design of big systems, where a number of equal-sized modules are mounted on the board with a regular placement pitch. A brief account of such knowledge base is given below, with an intention to provide some conceptual guides for designers of small systems as well.

Figure 3.11 presents a collection of the curves of heat transfer coefficient (h) versus the air velocity (U). The data "single module" was reported by Chang, Shyu, and Fang [2], with a single heated block measuring $6 \times 6 \times 2$ cm ($b/l = 1/3$) in a channel having a relative height $H/b = 3$. The curve "sparse flat packs" correlates the data obtained by Wirtz and Dykshoorn [20]. Their model of flat pack (block) had a

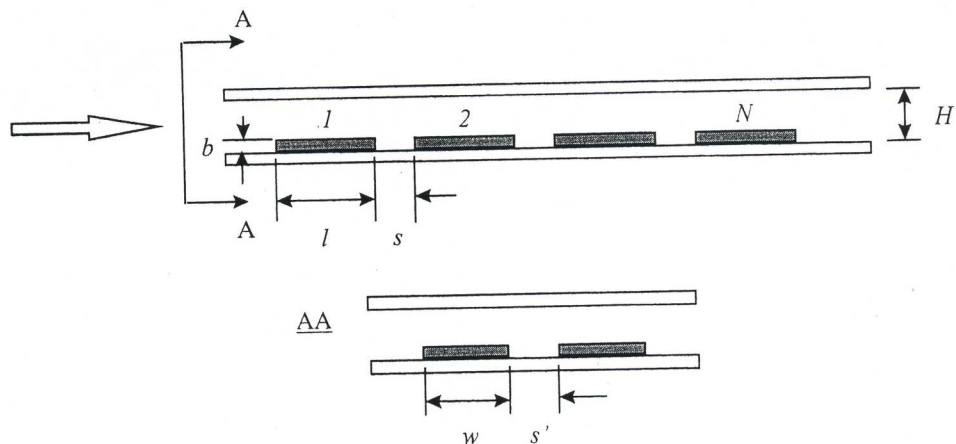


Figure 3.10 Module array on board.

h [$W/m^2 K$]

Figure
cooling

dim
par
cor
[19
ing
dat
sho
flat
dra
of a
fol

1.
2.

TABLE 3

Coolant
Air
FC77
Water

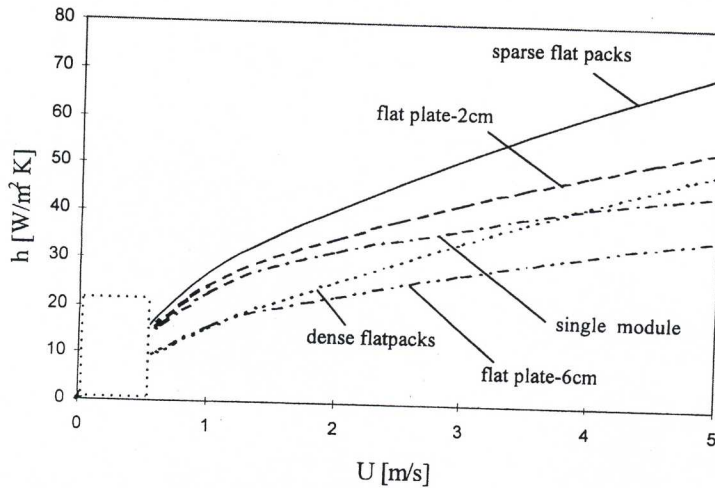


Figure 3.11 Typical heat transfer coefficients for forced convection air cooling of modules and flat plates.

dimension $2.54 \times 2.54 \times 0.64\text{cm}$, hence, the ratio $b/l = 0.23$. Other parameters were $H/b = 3.6$ and $s/l = 1$. The curve “densely flatpacks” correlates the data obtained by Sparrow, Neithammer, and Chaboki [19]. The block was $2.667 \times 2.667 \times 1\text{cm}$, and placed in a channel having $H/b = 2.67$. The spacing between the blocks was $s/l = 0.25$. Those data and correlations were discussed by Moffat and Ortega [15]. Also shown in Fig. 3.11 are the curves for heat transfer from a 2.54-cm-long flat plate (“flat plate-2cm”) and a 6-cm-long flat plate (“flat plate-6cm”), drawn using the first formula of Table 3.3 and the physical properties of air listed in Table 3.4. What we see in Fig. 3.11 are interpreted as follows.

1. The smaller the size of the module, the higher the heat transfer coefficient. See the sparse flatpacks and the flat plate-2cm versus the single module and the flat plate-6cm.
2. The coolant stream in the channel is accelerated where the module partially blocks the channel. Acceleration of coolant flow has an

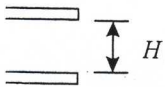
TABLE 3.4 Thermophysical Properties of Single-Phase Coolant at 300K

Coolant	Density, ρ [kg/m ³]	Specific heat, c_p [kJ/kg K]	Kinematic viscosity, ν [10 ⁻⁶ m ² /s]	Thermal conductivity, λ [W/m K]	Thermal diffusivity, κ [10 ⁻⁶ m ² /s]	Prandtl number, Pr	Coeff. thermal expansion, β [K ⁻¹]
Air	1.16	1.00	15.9	0.0263	22.5	0.7	0.0033 (300K)
PC77	1590	1.17	0.28	0.057	0.03	9.25	0.0014
Water	1000	4.18	0.86	0.613	0.15	5.7	0.00028

the appli-
al interest

from the
g. 3.10. In
(width)],
between the
location of
entrance of
situation is
ly in small
and other
nent data
; systems,
board with
ge base is
guides for

ansfer coef-
odule” was
ted block
ive height
tained by
k) had a



effect of reducing the boundary layer thickness, thereby increasing h . The flat plate formula gives h for the plate in open space; hence, its underprediction of h compared to the sparse flat packs and the single module performance partly reflects the effect of flow acceleration. A similar effect of flow acceleration is brought by the development of boundary layer on the upper channel wall, which displaces the coolant toward the center of the channel.

3. Where the modules are sparsely populated, the flow separated behind the module is developed into a turbulent wake before it reaches the next module. The increased level of turbulence is effective in producing high h . This partially explains the difference between the dense flatpacks and the sparse flatpacks.
4. Where the modules are densely packed on the board, coolant masses are trapped between the modules, and the front and back surfaces of the module do not serve as effective heat transfer surfaces. This may also be attributed to the difference between the sparse flatpacks and the dense flatpacks.
5. The preceding observations in (2), (3), and (4) lead us to consider how the location of the module affects h . Where the causes (2) and (3) prevail, the heat transfer coefficient (h_n) tends to increase on downstream rows (increasing n). On the other hand, where the cause (4) prevails, h_n decreases with increasing n . In any circumstances, however, it has been proved that the variation of h_n becomes practically negligible after the second or third row.

The heat transfer coefficient discussed earlier relates the heat flux to a temperature difference between the module surface and the coolant over the module; namely, T_∞ in Θ_∞ of Eq. 3.25 is the temperature of the coolant just outside the boundary layer developed on the module of interest. This temperature may be called *local free stream temperature*. The local free stream temperature increases as the coolant picks up heat from the modules in a row. Its increase from the inlet of the channel to the location of the N th module is

$$(\Delta T)_{\text{mix}} = \frac{1}{c_p M} \sum_{n=1}^{N-1} Q_n \quad [\text{K}] \quad (3.27)$$

where c_p [J/kg K] is the specific heat at constant pressure of the coolant, M [kg/s] is the mass flow rate of the coolant per column of the modules, and Q_n [W] is the heat dissipation rate of the n th module.

The term $(1/c_p M)$ is the equivalent thermal resistance, as noted in regard to Fig. 3.2c and Eq. 3.8. This thermal resistance, however, has to be amplified by a certain factor to account for imperfect mixing of the

coolant
is the
ough
ures
respe
temp
The c
wake.
Nth m
as

where
wake
transf
respec
The va
the up
and th
 σ has
right-h
reason
over a
viewed
of cons
as 2 to



Figure 3.12
mal wake

coolant in the channel. Namely, Eq. 3.27 holds only where the coolant is thoroughly mixed. In actual circumstances the coolant is never thoroughly mixed, but has a temperature distribution in the channel. Figures 3.12a and b depict thoroughly mixed flow and actual flow, respectively. Figure 3.12b shows T_∞ for the N th module ($T_{\infty,N}$), and the temperature distribution in the boundary layer on the N th module. The coolant mass of relatively high temperature is called *thermal wake*. We write the difference between the surface temperature of the N th module ($T_{s,N}$) and the coolant temperature at the channel inlet (T_0) as

$$T_{s,N} - T_0 = \Delta T + (T_{s,N} - T_{\infty,N}) \quad (3.28)$$

$$\Delta T \equiv T_{\infty,N} - T_0 = \sigma (\Delta T)_{\text{mix}} \quad (3.29)$$

$$T_{s,N} - T_{\infty,N} = \frac{Q_N}{h_N A_N} \quad (3.30)$$

where σ is the multiplying factor to account for the effect of thermal wake on the local free stream temperature, h_N and A_N are the heat transfer coefficient and the heat transfer area on the N th module, respectively, and Q_N is the heat dissipation rate from the N th module. The value of σ depends on several factors such as the distance between the upstream heat sources and the N th module, the coolant velocity, and the level of turbulence. When these factors are taken into account, σ has to be a function of n , and placed inside the summation on the right-hand side of Eq. 3.29. However, for the sake of brevity and with reasonable accuracy, we assume that σ is constant over the modules over a row of modules. Figure 3.13 shows a thermal resistance network viewed from the N th module to the channel inlet with the assumption of constant σ . For a conservative estimate, σ may be assumed as high as 2 to 3.

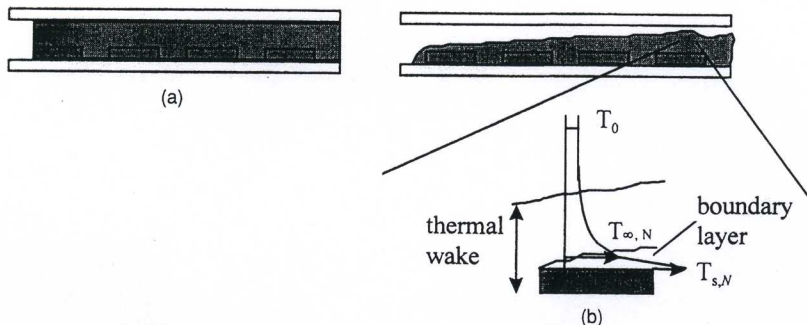


Figure 3.12 Mixing of warm air with free stream; (a) perfectly mixed flow; (b) thermal wake.

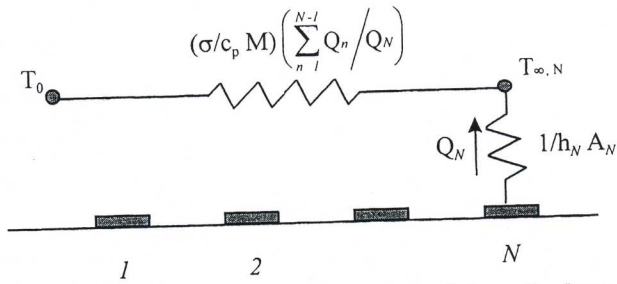


Figure 3.13 Thermal resistance from the module on the downstream row to the inlet air.

3.2.8 Conjugate heat transfer on heat spreader

Heat transfer at the board level is made even more complex if a significant portion of heat is conducted from the module to the board. The heat from the module spreads in the board and is eventually transferred to the coolant from the upper and lower surfaces of the board. The effect of the board as a heat spreader is particularly large, where the number of high-power modules is one or a few, and the back side of the board is exposed to the coolant. Heat conduction inside the board and convective heat transfer on the surface of the board are coupled in what we call *conjugate mode* of heat transfer. Similar conjugate heat transfer problems exist, where heat spreaders by design are attached to chips or modules.

Figure 3.14 shows a model of the heat spreader, where the heat source and the spreader are both replaced by circular disks having respectively equal surface areas; the heat source disk has a radius a ,

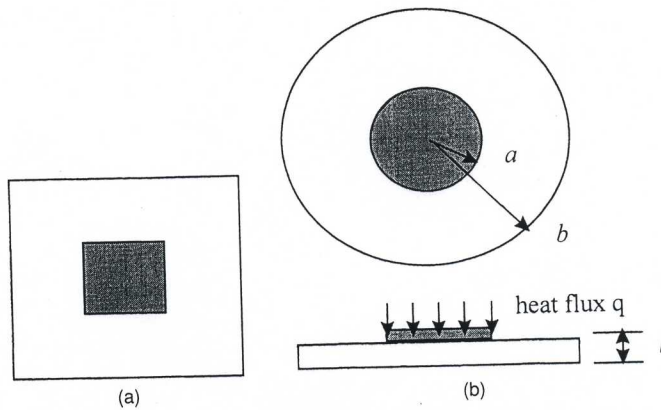


Figure 3.14 Convection-cooled heat spreader; (a) chip or module on heat spreader; (b) circular model.